Tetrafluorinated versus hydrogenated azobenzene polymers in water: Access to visible-ligh stimulus at the expense of responsiveness

Camille Courtine, Pierre-Louis Brient, Inès Hamouda, Nicolas Pataluch, Pierre Lavedan, Jean-Luc Putaux, Camille Chatard, Céline Galès, Anne-Françoise Mingotaud, Nancy Lauth de Viguerie, et al.

Tetrafluorinated versus hydrogenated azobenzene polymers in water: access to visible-light stimulus at the expense of responsiveness

Camille Courtine[a], Pierre-Louis Brient[b], Inès Hamouda[c], Nicolas Pataluch[d], Pierre Lavedan[e], Jean-Luc Putaux[f], Camille Chatard[b], Céline Galès[d], Anne-Françoise Mingotaud[a], Nancy Lauth-de Viguerie[a,*] and Erwan Nicol[c,*]

a. Laboratoire des IMRCP, Université de Toulouse, CNRS UMR 5623, Université Toulouse III - Paul Sabatier, 118 Rte de Narbonne, 31062 Toulouse cedex 9, France.

b. Specific Polymers, ZAC Via Domitia, 150 Avenue des Cocardières, 34160 Castries, France.

c. Institut des Molécules et Matériaux du Mans (IMMM), UMR CNRS 6283, Equipe Polymères, Colloïdes, Interfaces, Le Mans Université, Avenue Olivier Messiaën 72085 Le Mans Cedex 9, France

d. Institut des Maladies Métaboliques et Cardiovasculaires (I2MC), INSERM UMR 1297, Université Toulouse III - Paul Sabatier, 1 avenue Jean Poulhès - BP 84225 - 31432 Toulouse Cedex 4, France

e. Paul Sabatier University - Toulouse III | UPS Toulouse · Institut de Chimie de Toulouse ICT - FR 2599

f. Univ. Grenoble Alpes, CNRS, CERMAV, F-38000 Grenoble, France

E-mail addresses: nancy.de-viguerie@univ-tlse3.fr, erwan.nicol@univ-lemans.fr

Corresponding authors: Nancy Lauth-de Viguerie and Erwan Nicol

Tel: (33) 561 55 61 35 or (33) 243 83 33 62

Abstract

Photo-responsive polymers are at the core of numerous applications as actuators in biology but often exhibit the drawback of activation in the UV range. This work describes a methacrylate-based terpolymer presenting tetra-*ortho*-fluoroazobenzene groups showing activation through visible light illumination. The presence of poly(ethylene oxide) side chains and maleimide functions ensures that it can be easily used for biological applications in aqueous media. The terpolymer was shown to form unimolecular micelles in water. The tetra-*ortho*-fluoroazobenzene moiety was reversibly switched from *trans* to *cis* upon visible light irradiation without significant modification of the unimolecular morphology. The deprotection of the maleimide function resulted in a reactive polymer which was used to obtain hydrogels by reaction with poly(ethylene oxide) tetra-thiols or bioconjugates by reaction with a model peptide or a poly(ethylene oxide) mono-thiol exhibiting a biotin group. Hydrogels incorporating β-cyclodextrin molecules were also obtained. Contrary to polymers bearing hydrogenated azobenzenes, the terpolymer bearing tetra-*ortho*-fluoroazobenzene moieties did not form a complex with β-cyclodextrin and none of the presented hydrogels exhibited macroscopic changes upon irradiation although the *trans*/*cis* isomerization occurred. This was explained by the burial of tetra-*ortho*-fluoroazobenzene groups towards the polymer backbone, therefore completely hindering its access.

Keywords

Azobenzene – photoswitch – polymer – maleimide – self-assembly – hydrogel

1. Introduction

Stimuli-responsive systems have undergone extensive development based either on small molecules or polymers. Among all the stimuli available, light remains one of the most popular due to its non-invasiveness and ease of implementation. Beside applications in optics, electronics or microfluidics, stimuli-responsive systems are also explored in biology, acting as soft actuators or drug delivery systems [1]. Indeed, most light-responsive chemical groups are activated by UV light, the synthesis of chemical entities responding to visible light being often difficult and time-consuming [2]. Azobenzenes (AZO) are one of the most extensively studied classes of photoswitches, and have been incorporated into various light-responsive polymers. The AZO moiety exists in either a *cis* or *trans* configuration with respect to the N=N double bond. Transition from the *trans* to the *cis* isomer typically occurs under UV excitation while the reverse process can be achieved using either visible illumination close to 400 nm or simply waiting for thermal return [1]. AZO-bearing molecules and polymers have already been extensively developed [3-5], even in water in spite of the relative hydrophobicity of the AZO moieties. Several studies investigated their ability to self-assemble in aqueous solutions and their resulting organization under UV light irradiation [6-8]. Because *trans*-AZO and *cis*-AZO may form inclusion complexes of different affinity constants in various molecules such as cyclodextrins or cucurbiturils, they have been extensively assessed as phototunable systems. Typical applications are for drug release, self-healing or artificial muscles [9-11]. They have also been often incorporated in hydrogels, either on their own [12-13] or encapsulated in host-guest systems [14-17].

Starting from the fully hydrogenated AZO, it is well known that a modification of the phenyl ring substituents leads to modifications of the UV-visible absorbance spectra. The introduction of substituents in the *ortho* positions such as amino, (thio)ethers or halides has been shown to shift the absorbance bands to the visible range, to possibly increase the difference between *cis* and *trans* n-π* transition bands and slow down the thermal return to the *trans* form [12, 18-23]. The response in the visible range is especially essential for *in vivo* uses. The separation of *cis* and *trans* n-π* transition bands allows specific activation of either the *trans* or the *cis* isomer, therefore leading to photostationary states (PSS) with a higher content of each form. In this regard, the tetra-*ortho*-methoxy AZO has been assessed in several visible-activated systems, including layer-by-layer devices [24], amphiphilic systems that respond to both light and temperature [22] and hydrogels [25]. A concern still under debate is the stability of the substituted azobenzene moieties in biological media, especially for tetra-*ortho*-methoxy AZO [19, 26]. From a general standpoint, the choice of the AZO type has to be reasoned based on different parameters: wavelength of stimulation, isomeric ratio at the PSS, thermal stability of the *cis* form, stability in the medium for the final use and relative ease of synthesis. Each substituted AZO therefore exhibits assets and drawbacks. Among the existing possibilities, tetra-*ortho*-fluoro AZO, developed by Bléger and coll. [12, 20-21], presents the advantage of an accessible synthesis, irradiation wavelengths in the visible range (*trans* to *cis* transition around 530 nm and *cis* to *trans* transition close to 400 nm), and an increased stability of the *cis* form leading to a slow thermal return from the *cis* to the *trans* isomer. This has enabled the development of new phototunable muscarinic acetylcholine receptor agonists [27] or photo-responsive chlorine ion transports across biological membranes [28].

The tetra-*ortho*-fluoro AZOs have moved from small molecules to polymeric structures and have been assessed either on their own [3] or as inclusion complexes [29]. Bléger and coll. also described a chaotic actuator based on the activation of tetra-*ortho*-fluoro-AZO by sunlight [30] or the modulation of elastic modulus of a hydrogel using visible light [12]. However, examples remain limited and this might be linked either to the difficult synthesis linking AZO to other

functional moieties or to difficulties emerging from the intrinsically hydrophobicity of tetra-*ortho*-fluoro AZO molecules, especially when seeking applications in water.

In this aim, we designed a multi-functional terpolymer bearing tetra-*ortho*-fluoro azo groups and maleimide functions allowing cross-linking or chemical functionalization. We investigated its self-assembly in water, its ability to complex with β-cyclodextrin as well as its use for forming bioconjugates and hydrogels. We compared these properties to those of similar hydrogenated azo-based small molecules and polymers reported in the literature.

2. Materials and Methods

2.1. Reagents

Methacryloyl chloride was distilled under reduced pressure before use. 1,4-Dioxane and dimethylsulfoxide (DMSO) were dried over activated molecular sieves for at least 24 h before use. All other commercial reagents and solvents were used as received. DMSO, 2,5-dimethylfuran, methacryloyl chloride, poly(ethylene glycol) methacrylate MPEO-MA with 19 EO units (MW = 950 g.mol^{-1}), triphenylphosphine, absolute ethanol, tetra-thiol-PEO 5k, were purchased from Sigma-Aldrich. Diethyl azodicarboxylate (DEAD, 40 % in toluene) was purchased from Alfa Aesar. 2-(dodecylthiocarbonothioylthio)-2-methylpropionic acid (DDMAT) was purchased from TCI Chemicals. 1,4-Dioxane was purchased from VWR Chemicals. Deuterated chloroform, deuterium water (D_2O) and deuterated dimethylsulfoxide (DMSO-d_6) were purchased from Eurisotop. Maleimide was purchased from Apollo Scientific. 2,2'-azobis(4-methoxy-2,4-dimethylvaleronitrile) (V-70) was purchased from Fujifilm Wako Chemicals.
Tetra-*ortho*-fluoro AZO hydroxyl-terminated PEO (4FAZO-PEO-OH) (7.3 EA units, MW = 590 g.mol^{-1}) was obtained from the Synthesis platform of ICBMS in Lyon, following already described procedures (scheme S1).[31] The peptide GCREIPESLRAGERC (M = 1676 g.mol^{-1}) was obtained from NeoBiotech. Biotin-PEO-SH (M = 790 g.mol^{-1}) was purchased from Iris Biotech. Ultrapure water was obtained from PURELAB flex 1 Dispenser from ELGA LabWater. All syntheses involving the AZO derivatives were performed in the dark.

2.2. Synthesis procedures

Synthesis of 4F-AZO-PEO-MA (scheme S2.1)*:* 4F-AZO-PEO-OH (9.50 g, 16.4 mmol, 1 eq) was dissolved in dichloromethane (100 mL) in a two-neck round-bottom flask. Triethylamine (2.83 g, 27.9 mmol, 1.7 eq) was then added. The mixture was then cooled down to 0°C using an ice bath. Methacryloyl chloride (2.58 g, 24.7 mmol, 1.5 eq) was then added dropwise under argon flow. Once the addition was complete, the ice bath was carried off and the mixture was left under stirring at room temperature during 2 h. The mixture was diluted 5-fold by adding 400 mL of dichloromethane. Afterwards, the solution was successively washed with 50 mL aqueous hydrochloric acid solution at 0.5 mol.L^{-1}, twice with 50 mL of aqueous sodium hydroxide solution at 1 mol.L^{-1} and last with 50 mL of deionized water. The organic phase was dried over anhydrous sodium sulfate, then concentrated by vacuum evaporation until complete solvent removal. 4F-AZO-PEO-MA was obtained as an orange viscous wax (9.9 g, yield: 93%). ^{1}H, ^{13}C and ^{19}F NMR spectra are shown in Fig. S1.
^{1}H NMR (300 MHz, $CDCl_3$) δ (ppm): 7.32 (m, 1H), 7.05 (t, 2H, *J* = 8.7 Hz), 6.64 (d, 2H, *J* = 11.1 Hz), 6.13 (s, 1H), 5.58 (s, 1H), 4.31 (t, 2H, *J* = 4.9 Hz), 4.20 (t, 2H, *J* = 4.6 Hz), 3.89 (t, 2H, *J* = 4.7 Hz), 3.55-3.82 (m, 24H),1.95 (s, 3H). MW=675 g/mol (7.7 EO units)

^{13}C NMR (75 MHz, $CDCl_3$) δ (ppm): 167.34, 161.88, 159.12, 157.22, 155.66, 153.78, 136.16, 132.08, 130.40, 126.08, 125.71, 112.65, 99.69, 70.94, 70.63, 69.24, 68.56, 53.87, 18.29.
The 4F-AZO-PEO-MA obtained was characterized by Steric Exclusion Chromatography (SEC) and the average molecular number (M_n), weight (M_w) and the polydispersity (PDI) are as the following:
SEC-DMF: M_n(eq-PEO) = 505 g.mol^{-1}, M_w(eq-PEO) = 550 g.mol^{-1}, PDI = 1.09

Synthesis of dimethylfuran-blocked maleimide: Maleimide (20.0 g, 0.206 mol, 1.0 eq) and 2,5-dimethylfuran (33.7 g, 0.350 mol, 1.7 eq) were dissolved in 240 mL of deionized water in a round-bottom flask. The mixture was left under stirring at room temperature for 5 days. The white precipitate was filtered on a frit (porosity 4) and washed twice with 200 mL of deionized water. The powder was then dried over phosphorus pentoxide in a desiccator under vacuum at room temperature. Dimethylfuran-blocked maleimide was obtained as a white powder (39.8 g, yield: 75%).
^{1}H and ^{13}C NMR spectra are shown in Fig. S2.
^{1}H NMR (300 MHz, $CDCl_3$) δ (ppm): 8.15 (bs, 1H), 6.22 (s, 2H), 3.21 endo – 2.81 exo (s, 2H), 1.71 endo – 1.65 exo (s, 6H).
^{13}C NMR (75 MHz, $CDCl_3$) δ (ppm): 175.66, exo 140.88, endo 138.18, 87.93, endo 54.90, exo 53.83, endo 18.54, exo 15.78.

Synthesis of MALp-PEO-MA (scheme S2.2): Poly(ethylene glycol) methacrylate HO-PEO-MA (n=9.5; MW=500 g.mol^{-1}) (26.8 g, 51.8 mmol, 1.0 eq) was dissolved in anhydrous tetrahydrofuran in a two-neck round-bottom flask. Dimethylfuran-blocked maleimide (20.0 g, 0.104 mol, 2.0 eq) and triphenylphosphine (31.2 g, 0.119 mol, 2.3 eq) were then added. The mixture was cooled down to 0°C using an ice bath, and diethyl azodicarboxylate (DEAD), 40 % in toluene, was added dropwise. After the addition was complete, the ice bath was carried out and the mixture was left under stirring overnight at room temperature.
The solvents were eliminated by vacuum evaporation. The resulting oily product was dissolved in 150 mL of diethyl ether and then extracted twice with 250 mL of deionized water. The aqueous phases were combined and extracted twice with 950 mL of dichloromethane. The combined organic phase was dried over anhydrous sodium sulfate. After evaporating the solvent, the orange oily residue was purified by silica-gel flash column chromatography using dichloromethane: methanol (90 / 10 vol %) as solvents.
MALp-PEG-MA was obtained as an orange viscous (9.0 g, yield: 25 %).
^{1}H and ^{13}C NMR spectra are shown in Fig. S3.
^{1}H NMR (300 MHz, $CDCl_3$) δ (ppm): 6.21 (s, 2H), 6.14 (s, 1H), 5.58 (s, 1H), 4.30 (t, 2H, J = 4.7 Hz), 3.49-3.78 (m, 60H), 3.22 (s, 2H), 1.95 ppm (s, 3H), 1.79 ppm (s, 6H). MW=950 g/mol (15.6 EO units)
^{13}C NMR (75 MHz, $CDCl_3$) δ (ppm): 175.07, 167.32, exo 140.89, endo 137.99, 136.14, 125.70, 87.89, 70.54, 69.85, 69.12, 67.02, 63.86, endo 53.44, exo 52.45, 37.56, endo 18.64, 18.28, exo 15.85.
The MAL-PEG-MA obtained was characterized by SEC and the M_n, M_w and the PDI are as the following:
SEC-DMF: Mn(eq-PEO) = 835 g.mol^{-1}, Mw(eq-PEO) = 1045 g.mol^{-1}, PDI=1.25

Synthesis of Poly(4FAZOPEOMA-co-MPEOMA-co-MALpPEOMA) ***1p****:* MPEO-MA with 19 EO units (MW=950 g.mol^{-1}) (6.0 g, 6.32 mmol, 18.8 eq), MALp-PEO-MA (3.2 g, 3.36 mmol, 10.0 eq), 4FAZO-PEO-MA (1.09 g, 1.69 mmol, 5 eq), DDMAT (0.122 g, 0.335 mmol, 1.0 eq) and V-70 (42.0 mg, 0.136 mmol, 0.4 eq) were introduced in a Schlenk flask and dissolved in 20 mL of *N*,*N*-dimethylformamide. The mixture was deoxygenated by three argon/vacuum

cycles at room temperature, then heated at 30°C during 29 hours. The polymerization was quenched by cooling down to 0°C using an ice bath with air exposure. The crude mixture was diluted in 240 mL of tetrahydrofuran and purified by dialysis (MWCO = 1 kDa). The dialyzed solution was then concentrated and precipitated in 240 mL of pentane/Et_2O (95:5 $_{v/v}$). After drying under vacuum at 30 °C, the terpolymer was obtained as an orange viscous oil (5.6 g, Yield: 55%). ^1H, ^{13}C, quantitative ^{13}C, COSY, HSQC, HMBC NMR spectra are shown in Fig. S4.

^1H NMR (500 MHz, $CDCl_3$) δ (ppm): 7.34 (m, -CF=CH-C<u>H</u>=CH-CF), 7.05 (t, -CF=C<u>H</u>-CH=C<u>H</u>-CF), 6.72 (s, -N-CO-C<u>H</u>=C<u>H</u>-CO(N) unprotected maleimide), 6.65 (d, -C<u>H</u>-CF=C($N_2C_6H_5F_2$)-CF=C<u>H</u>-), 6.32 (s, -CHO(CH_3)-C<u>H</u>=C<u>H</u>-CH(O)(CH_3)- exo), 6.22 (s, -CHO-C<u>H</u>=C<u>H</u>-CH(O)- endo), 3.43-4.32 (m, -O-C<u>H_2</u>-C<u>H_2</u>-O-), 3.39 (s, -O-CH_2-CH_2-O-C<u>H_3</u>), 3.22 (s, -N-CO-C<u>H</u>(C_6H_8O)C<u>H</u>-CO(N) endo) 2.84 (s, -N-CO-C<u>H</u>(C_6H_8O)C<u>H</u>-CO(N) exo), 2.10 (m, -C<u>H_2</u>- backbone), 1.79 (s, -C<u>H_3</u> endo), 1.71 (s, -C<u>H_3</u> exo), 1.22-1.4 (COOH-C(C<u>H_3</u>)$_2$- end-group, -(C<u>H_2</u>)$_{10}$-CH_3 end-group), 0.6-1.22 (-C<u>H_3</u> backbone, -C<u>H_3</u> end-group).$M_{n,NMR}$=20,000 g/mol (14.3 MPEOMA units, 4.1 MALPEOMA units, 3.4 AZOPEOMA units).

^{13}C NMR (125 MHz, $CDCl_3$) δ (ppm): 177.41, 175.10, 174.69, 170.67, 161.92, 158.41, 158.35, 156.47, 156.33, 156.27, 154.41, 140.91, 138.02, 135.77, 130.47, 112.63, 112.47, 99.85, 99.67, 99.65, 99.46, 87.91, 87.58, 71.93, 70.56, 70.04, 69.86, 69.25, 69.14, 68.63, 68.45, 67.83, 67.21, 64.12, 63.88, 69.14, 68.63, 68.45, 67.83, 67.21, 64.12, 63.88, 59.03, 53.46, 52.47, 44.85, 37.98, 37.57, 37.12, 34.22, 31.90, 29-29.8, 22.68, 19.59, 18.63, 15.89, 14.16.

SEC-DMF (Fig. S5): Mn(eq-PEO) = 15 400 g.mol^{-1}, Mw(eq-PEO) = 35 200 g.mol^{-1}, PDI=2.28

Deprotection of maleimide functions (retro-Diels-Alder reaction) ***1****:* 200 mg of poly(4F-AZO-PEO-MA-co-MPEOMA-co-MALpPEOMA) terpolymer were dissolved in 2 mL of dioxane in a two-neck round-bottom flask equipped with Dean-Stark glassware. The Dean-Stark part was filled with dioxane. The mixture was stirred during 4 hours at 93 °C under constant argon bubbling, to help the elimination of the dimethylfuran from the mixture. The remaining dioxane and free dimethylfuran were evaporated. The final product was dried under vacuum. The deprotected terpolymer was kept with precaution in the dark and under argon at –20 °C. The maleimide-polymer was obtained as an orange wax (195 mg, Yield: 95%). ^1H and ^{13}C NMR spectra of poly(4F-AZO-PEO-MA-co-MPEOMA-co-MALPEOMA) are shown in Fig. S6.

^1H NMR (300 MHz, $CDCl_3$) δ (ppm): 7.34 (m, -CF=CH-C<u>H</u>=CH-CF), 7.05 (t, -CF=C<u>H</u>-CH=C<u>H</u>-CF), 6.72 (s, -N-CO-C<u>H</u>=C<u>H</u>-CO(N)), 6.65 (d, -C<u>H</u>-CF=C($N_2C_6H_5F_2$)-CF=C<u>H</u>-), 3.43-4.32 (m, -O-C<u>H_2</u>-C<u>H_2</u>-O-), 3.39 (s, -O-CH_2-CH_2-O-C<u>H_3</u>), 2.10 (m, -C<u>H_2</u>- backbone), 1.22-1.4 (COOH-C(C<u>H_3</u>)$_2$- end-group, -(C<u>H_2</u>)$_{10}$-CH_3 end-group), 0.6-1.22 (-C<u>H_3</u> backbone, -C<u>H_3</u> end-group).$M_{n,NMR}$=19,600 g.mol^{-1}

^{13}C NMR (125 MHz, $CDCl_3$) δ (ppm): 177.32, 170.66, 160.20, 153.76, 153.69, 152.74, 151.69, 150.70, 134.19, 129.45, 112.62, 112.62, 112.45, 112.18, 112.04, 99.84, 99.46, 99.09, 98.89, 71.93, 70.56, 70.04, 69.23, 69.14, 68.43, 67.81, 67.08, 64.12, 63.88, 59.03, 44.85, 37.12, 31.90, 29.0-29.80, 27.18, 22.69, 19.59, 14.12.

2.3. NMR spectroscopy

^1H, ^{13}C and ^{19}F NMR experiments were performed at 298 K using a Bruker AVANCE spectrometer at 300 MHz for ^1H and 75 MHz for ^{13}C or a Bruker AVANCE 500MHz spectrometers equipped with a 5 mm Z-gradient TCI cryoprobe and with a 5 mm Z-gradient PRODIGY cryoprobe or using a Bruker Advance 400 MHz (^1H, NOESY) spectrometer. The terpolymer was dissolved in deuterated solvents (D_2O and DMSO-d_6) to a final concentration of 20 mg.mL^{-1}. Dispersion from an organic solvent into an aqueous solution was performed by

dissolving the terpolymer in DMSO-d_6 at a concentration of 20 $_{wt}$%. Then D_2O was slowly added under stirring to a final ratio DMSO-d_6/D_2O of 1:10 and a final terpolymer concentration of 2 $_{wt}$%.

2.4. Size-exclusion chromatography

Size Exclusion Chromatography (SEC) measurements were performed on an Agilent Technologies 1260 infinity II system equipped with a refractive index detector, Polargel M columns (7.5 x 300 mm, 8 µm) at 80°C, using *N*,*N*-dimethylformamide as eluent at a flow rate of 1 mL·min^{-1}. The system was calibrated using PEO standards.

2.5. Spectroscopy

UV-visible spectroscopy was performed either on a HP 8452A Diode-Array spectrometer in a 1 cm pathlength quartz cuvette equipped with a magnetic stirrer, or a Varian Cary 100 Bio UV-Visible spectrometer equipped with a temperature controller from Varian Cary, spectrometer in a 1 cm pathlength quartz cuvette equipped with a magnetic stirrer. Two solutions at C=10 g.L^{-1} of *cis*-enriched terpolymer were prepared, one in ultra-pure water and the other in absolute ethanol. These solutions were diluted 4; 10; 20; 40; 100; and 200 times to study the effect of dilution. The most concentrated solutions were used to compare spectra in both solvents. The analyses were performed in quartz cuvettes.
Fluorescence measurements were performed with a Fluorolog TCSPS from Horiba Scientific in a 1cm pathlength quartz cuvette. Irradiations were performed using a LED system from Mightex® equipped with an optical fiber. The LEDs were used at their maximal power. A 0.2 g.L^{-1} solution of 4FAZO-PEO-OH and 2.7 g.L^{-1} solution of protected terpolymer in DMSO was prepared. Four sample solutions were prepared for each compound with 0, 100, 200 and 300 $_{v/v}$% of water added to the DMSO solutions. The solutions were excited at 373 nm and the fluorescence recorded between 400 and 700 nm with a slit of 6 nm for the 4FAZO-PEO-OH solutions and a 4-nm slit for the polymer solutions (Fig. S7).

2.6. Preparation of the terpolymer solutions

The behavior of the synthetized terpolymer was characterized in aqueous solutions after direct dissolution in water or using the "DMSO route". A solution was prepared at a concentration of 20 g.L^{-1} by dissolving the terpolymer in distilled water or in anhydrous DMSO. These solutions were then irradiated at 415 or 530 nm during 15 min in order to photo-switch in *trans* or *cis* configuration respectively. Terpolymer solutions were then diluted to 2 g.L^{-1} by adding distilled water, leading to a DMSO concentration < 10%, allowing thus their characterization in aqueous solution.

2.7. Light scattering

Apparent molar masses (M_a) and hydrodynamic radius (R_h) of terpolymer-AZO in solution were assessed by static (SLS) and dynamic (DLS) light scattering. Data were recorded with a ALV-5000 multibit (ALV-GmbH, Germany), multitau, full digital correlator in combination with a Spectra-Physics laser (emitting vertically polarized light at k = 632.8 nm) and a thermostat bath controlled at 20±0.2 °C. The measurements were made at angles (θ) ranging between 20 and 150°. Before measurement, the polymer solutions were filtered using 0.45 µm inorganic membrane filter. The sample concentration varied between 2 and 10 g.L^{-1} and the refractive index increment of the terpolymer in water was assumed as (dn/dC) = 0.155 mL.g^{-1}

which seems reasonable based on the very similar values for polymethacrylic-based polymers and in water.[32] The average relaxation rate (Γ) was found to be q^2 independent (where q is the scattering vector: $q = (4\pi n/k)/\sin(\theta/2)$). The cooperative diffusion coefficient (D_c) was calculated as: $D_c = \Gamma/q^2$. At sufficiently low concentrations, where interactions are negligible, the z-average apparent hydrodynamic radius (R_h) of the solute can be calculated from the diffusion coefficient (D_c) using the Stokes-Einstein relation:

$$R_h = \frac{k_B \times T}{6 \times \pi \times \eta_s \times D_c}$$

where k_B is the Boltzmann constant, T is the absolute temperature and η_s is the solvent viscosity. The relative excess scattering intensity (Ir) was determined as the total intensity minus the solvent scattering divided by the scattering of toluene at 20 °C. Ir is related to the osmotic compressibility ($(d\pi/dC)^{-1}$) and the z-average structure factor (S(q)):

$$Ir = K.C.R.T.(d\pi/dc)^{-1}\ S(q)$$

With R the gas constant and T the absolute temperature. In dilute solutions Ir is related to the weight average molar mass (M_w) and the z-average structure factor (S(q)):

$$Ir = K.C.M_w.S(q)$$

With C the solute concentration and K an optical constant that depends on the refractive index increment. S(q) describes the dependence of Ir on the scattering wave vector. For the concentrations studied (2 to 10 $g.L^{-1}$), interactions influence the scattering intensity and the result obtained by extrapolation to q = 0 represents an apparent value for the apparent molar mass (M_a).

2.8. Transmission electron microscopy

A droplet of the terpolymer dilute suspension (ca. 0.001 $_{wt}$%) was deposited on a carbon-coated copper grid freshly glow-discharge in a Pelco easiGlow station. The liquid in excess was blotted and, before drying, a droplet of 2 $_{wt}$% uranyl acetate negative stain was deposited. The stain in excess was absorbed and the preparation allowed to dry. The specimen was observed with a JEOL JEM-2100 Plus microscope operating at 200 kV and images were recorded with a Gatan Rio 16 camera (Fig. S8).

2.9. Hydrogel preparation

The hydrogel was prepared from the poly(4FAZOPEOMA-co-MPEOMA-co-MALPEOMA) terpolymer and a tetra-thiol-PEO (5000 $g.mol^{-1}$). The thiol content of the PEO was quantified by ^{1}H NMR spectroscopy as 0.75 $mmol.g^{-1}$. Solutions of unprotected terpolymer and tetra-thiol-PEO were prepared at the concentrations of 122.2 $g.L^{-1}$ and 80.0 $g.L^{-1}$ respectively. The hydrogel was formed by mixing the two solutions in volumic ratio 7:3 terpolymer:thiol. The mixture was then immediately molded in an inverted syringe of 10 mm diameter and left standing for one night at 4 °C protected from light.

2.10. Rheology

Rheological measurements were carried out at 25 °C with a stress-control rheometer MCR301 (Anton Paar, Austria) using a cone-plate geometry (CP: 25 mm, gap: 0.52 mm). The measurements were done in the linear response regime (f = 1 Hz and at 1 % of deformation). During the experiment, the sample was covered with mineral oil in order to avoid evaporation and the rheometer protected from light. The sample was exposed to a green and blue LED (Thorlabs – M530LP1 and M415LP1 respectively) equipped with a light guide (Ø = 5 mm) placed 5 cm below the glass plate. The samples were irradiated during 15 min with intervals of 30 min.

A peptide solution (0.1 $_{wt}$ %) was added to the terpolymer solution before mixing with the tetra-thiol-PEO in order to delay the cross-linking reaction to be able to transfer the mixture to the rheometer plate.

2.11. Uniaxial compression tests

Cylinders of hydrogels were prepared as described in section 2.9. Compression tests were carried out on a Bose Electroforce 3100 mechanical testing machine equipped with a 20 N loading cell. Prior to each measurement, the hydrogel sample's height (h_0) and diameter (d) were measured. The sample was compressed over 0.5 mm (<15 % strain) at a speed of 5 mm.s^{-1}. While recording the deformation (Δh), the force (F) applied on the sample is monitored by the apparatus. The resulting stress-strain curve of the hydrogel $\boldsymbol{\sigma}$= f(ε) is obtained according to the following equations (1 and 2).

$$\sigma = F/(\pi \cdot (d/2)^2) \quad (1)$$

$$\varepsilon = \Delta h/h\_0 \quad (2)$$

The Young modulus (E) is obtained by the original slope of the curve as $E=\sigma/\varepsilon$
E was extracted using a mathematical linear fitting from the first points of the curves (from 0 to 2% of strain as shown in Fig. S9).

2.12. Access to bioconjugates

Peptide grafting. Stock solutions of maleimide terpolymer **1** (S_{terpo}) and peptide (GCREIPESLRAGERC) ($S_{peptide}$) were prepared in deuterated water at concentrations of 47.5 g.L^{-1} and 50 g.L^{-1} respectively. S_{terpo} and $S_{peptide}$ were mixed in ratio 3:1 and poured into an NMR tube so that the final ratio between maleimide and thiols functional groups was 1:2 approximately. The mixture was then stirred at room temperature during 3 days and analyzed over time by ^{1}H NMR. After three days of stirring, the content of the tube was dialyzed during 5 days against distilled water at room temperature on a dialysis tube equipped with a 1 kDa cut-off membrane. The final product was obtained after freeze drying as an orange solid.
Biotin-PEO grafting: A stock solution (S_{terpo}) at 46.2 g.L^{-1} and another of biotin-PEO-SH (S_{biotin}) at 50.8 g.L^{-1} were prepared in deuterated water. S_{terpo} and S_{biotin} were mixed in a ratio 2:1 and poured into an NMR tube (with a final maleimide:thiol ratio around 1:3.5). The mixture was stirred at room temperature during 24 hours and analyzed over time by ^{1}H NMR.

3. Results and discussion

With the aim to assess visible light switchable tetra-*ortho*-fluoro azobenzene (4F-AZO) molecules for potential bio-application, we designed a multifunctional hydrophilic terpolymer. It exhibits a polymethacrylate backbone bearing oligo(ethylene oxide) pendant chains, some of which being functionalized with 4F-AZO or maleimide groups (scheme 1). The strategy was to ensure water solubility through the oligo(ethylene oxide) groups, bring photostimulation by the 4F-AZO and remaining reactive site with the maleimide functions for possible further use as hydrogels or bioconjugates [33]. We compare in this work terpolymer **1** and two small molecules bearing either hydrogenated [34] (AZO-H-PEO) or tetra-*ortho*-fluorinated [35] AZO (4F-AZO-PEO) (scheme 1).

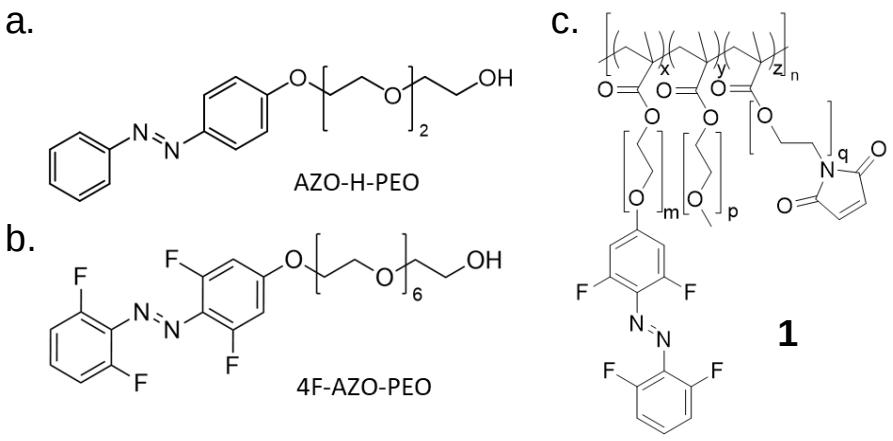

Scheme 1. Chemical structures of a) AZO-H-PEO, b) 4F-AZO-PEO and c) terpolymer **1**.

3.1 Synthesis of the multi-functional terpolymer

The first step consisted in synthesizing a hydrophilic copolymer incorporating both AZO groups together with maleimide ones in order to provide further reactivity (scheme 2). Terpolymer **1p** synthesis was performed by reversible addition-fragmentation chain transfer (RAFT) polymerization at 30°C using three corresponding monomers (Scheme 2, Fig. S1 and Fig. S2): *ortho*-fluorinated AZO PEO methacrylate (4F-AZO-PEO-MA) (m=7.3; Mn=590 $g.mol^{-1}$)[31], dimethylfuran-blocked maleimide PEO methacrylate (MALp-PEO-MA) (q=9.5; Mw = 500 $g.mol^{-1}$) and a commercial poly(ethylene oxide) methyl methacrylate (MPEO-MA) (p=19; Mw = 950 $g.mol^{-1}$). The protection of the maleimide group aimed to prevent side reactions throughout the polymerization process. Obtaining the terpolymer while preserving the integrity of the protected maleimide groups and avoiding premature formation of gels proved to be extremely difficult. Among other controlled radical polymerization methods, Activators ReGenerated by Electron Transfer Atom Transfer Radical Polymerization (ARGET ATRP) was first explored.[36-37]. We anticipated that the polymerization temperature might be a central point to consider, owing to the temperature-sensitive maleimide protection group and ARGET ATRP enabled to work at low temperature. The ATRP technique involves a catalytic process using a metal complex between a transition metal ion and coordinating nitrogen-based ligands. In ARGET ATRP, copper catalyst can be added initially as Cu(II) and generate active Cu(I) in situ via reduction at the start of the polymerization. Therefore, the catalyst precursors are not air-sensitive, and require less stringent deoxygenation conditions. Experimental parameters are given in Table S1. The results showed that it was not possible to find adequate conditions: either the polymerization yield was low (maximal conversion rate of 54% was reached after 22 hours of reaction at 30°C) or insoluble gel formation was observed before the end of the reaction.

This result led us to re-examine the choice of the controlled polymerization technique and examine RAFT conditions which would allow to simplify the purification stage, as the only impurities to remove would be the residual monomers. RAFT in usual conditions using azobisisobutyronitrile at 70 °C resulted in side reactions linked to premature deprotection of maleimide groups. Only the RAFT polymerization at 30 °C using a

trithiocarbonate as RAFT agent allowed a hydrophilic protected terpolymer (Mn = 15 400 g.mol^{-1} eq PEO, Fig. S5) to be obtained containing both protected maleimide (≈ 4.5 units) and azobenzene groups (≈ 4.9 units).

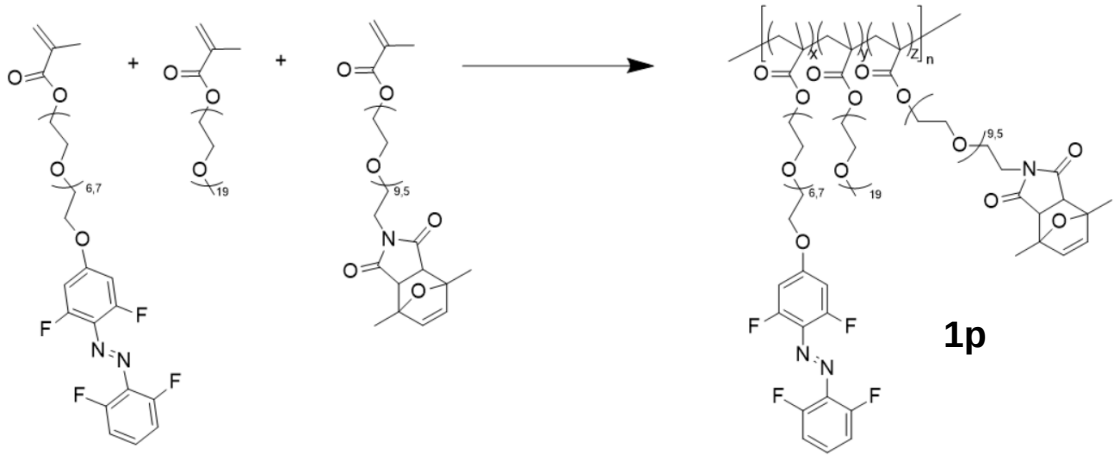

Scheme 2. Formation of hydrophilic terpolymer **1p** bearing tetra-*ortho*-fluoro AZO groups by RAFT polymerization at 30°C in DMF using V-70 as initiator and 2-(dodecylthiocarbonothioylthio)-2-methylpropionic acid as chain transfer agent.

Many examples of AZO-bearing polymers have been described in the literature, some of which are presented in Table S2. They are typically obtained from two different strategies, either radical polymerization using an AZO-bearing monomer [38-44], or the post-modification of a preformed polymer [24, 45-52]. The polymer main chain is either based on polysaccharides such as carboxymethylcellulose [45] or hyaluronic acid [47] or synthetic polymers like poly(acrylic acid) [46, 48-49] or poly(N-isopropyl acrylamide)[42]. The chemistry involving the AZO parts are all comparable, since in all cases a spacer is present between the AZO moiety and the polymer backbone. This is also true for terpolymer **1p** in which the tetra-*ortho*-fluorinated AZO is inert during the polymerization, consistent with several examples of radical polymerization of fluorinated monomers such as fluorostyrene [53-55]. However, terpolymer **1p** presents the challenge of the presence of the maleimide groups and their inherent reactivity, even in their protected form. The difficulty of obtaining the terpolymer **1p** directly comes from these maleimide groups and not from 4F-AZO.

3.2 Photoresponsive behavior in water

The UV-visible spectra of all three molecules of Scheme 1 in their *cis* and *trans* photostationnary states (PSS) are presented in Fig. 1a and 1b. The comparison between the absorption spectra of the PSS $(415)_{trans}$ and $PSS(530)_{cis}$ of the 4F-AZO on the protected terpolymer shows that the π→π* band is less intense for the *cis* isomer, which is common for azobenzenes. The positions of the maxima (Table 1) confirmed that the fluorinated AZO is more suitable for selective illumination of each state compared to the hydrogenated AZO. Indeed, there is a strong difference in the *cis* and *trans* form spectra above 480 nm, meaning that the n→π*could be used to selectively trigger the *cis* to *trans* isomerization.

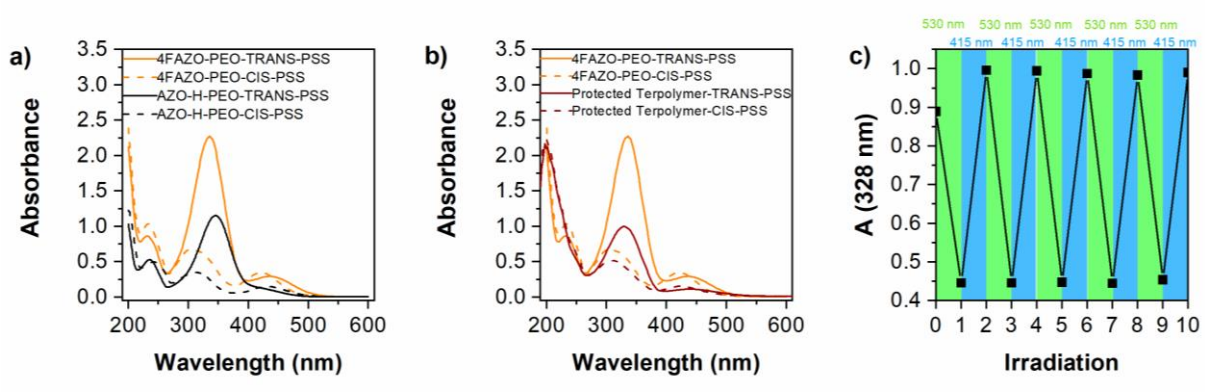

Fig. 1. Absorption spectra in water of a) $PSS(530)_{cis}$ (orange dotted lines), $PSS(366)_{cis}$ (black dotted lines and $PSS(415)_{trans}$ (solid lines) for 4F-AZO-PEO and AZO-H-PEO ([AZO] = 5.10^{-5} mol.L^{-1}) and b) $PSS(530)_{cis}$ (dotted lines) and $PSS(415)_{trans}$ (solid lines) for 4F-AZO-PEO and the protected polymer ([AZO] = 5.10^{-5} mol.L^{-1} and [terpolymer] = 2 g.L^{-1}). c.) Illumination cycles of the terpolymer **1** showing a good stability.

Table 1. Maxima of the n→π* absorption band of *trans* and *cis PSS*s of the studied azobenzenes and the protected polymer **1p**.

Compound	Solvent	Configuration	n→π* λ_{max} (nm)
AZO	$CDCl_3$	*trans*	445
		cis	440
AZO-H-PEO	H_2O	*PSS(415)trans*	-
		PSS(366)cis	430
4F-AZO-PEO	H_2O	*PSS(415)trans*	436
		PSS(530)cis	422
Protected terpolymer **1p**	H_2O	*PSS(415)trans*	436
		PSS(530)cis	424

The unprotected terpolymer **1** in solution in water was consecutively irradiated at 415 and 530 nm until reaching its PSS (Fig. 1c). From the absorbance at 328 nm, it is shown that green and blue lights respectively triggered *cis* and *trans* isomerizations respectively. Moreover, the terpolymer photo-switch did not undergo any fatigue after 5 cycles. The PSS_{cis} (19 % *trans*:81 % *cis*) of the terpolymer was reached after 3 min irradiation at 530 nm (P=30 mW.cm^{-2}) while the PSS_{trans} (72% trans:28% cis) was obtained after 1 min irradiation at 415 nm (P = 90 mW.cm^{-2}).

Comparatively, we showed that the $PSS(530)_{cis}$ and $PSS(415)_{trans}$ values for the 4F-AZO-PEO in the same conditions were 72 % *cis* and 67 % respectively for the *cis* and the *trans* [35]. Thus the terpolymer exhibited enriched PSSs compared to the small molecule. For H-AZO-PEO the $PSS(530)_{cis}$ was not able to be determined owing to extremely low absorbance at this wavelength. The $PSS(420)_{trans}$ was measured after irradiation at 366 nm and found at 60 %, [34] which is the lowest value of the three considered molecules.

3.3 Organization of the tetra-ortho-fluoro AZO molecules in water

Both 4F-AZO-PEO and terpolymer **1** can be considered as amphiphilic molecules, owing to the hydrophilic PEO chains and the hydrophobic fluorinated AZO groups, together with the polymethacrylate main chain for the polymer. Furthermore, the presence of oligo(ethylene oxide) chains could result in a precipitation of the molecule above a cloud point linked to a lower critical solution temperature (LCST) behavior. This phenomenon has been extensively described in the literature [56-57]. Turbidimetry measurements at different temperatures showed that the terpolymer did not exhibit any cloud point up to 55 °C, contrary to 4F-AZO-PEO which precipitated above 25 °C (Fig. S10) [35]. All subsequent experiments were thus conducted at room temperature.

We formerly showed that 4F-AZO-PEO exhibits a critical aggregation concentration at 1.5 mM at 4°C either in the *cis* or *trans* state [35]. The formation of terpolymer **1p** self-assemblies in water was first assessed by UV-visible spectroscopy. AZO aggregation is usually illustrated by a shift of the absorption bands of the dye and their broadening.[58] When the terpolymer absorption spectrum was recorded in water, a bathochromic shift of 2 nm was observed compared to the same solution in ethanol (Fig. S11a). The shift did not seem large enough to be aggregation-related. It is most likely linked to a solvatochromic effect due to the increased polarity of water vs ethanol. This was also pointed by the absence of evolution of the spectrum upon dilution in water, although this is not a proof (Fig. S11b). We further investigated the potential of an aggregation phenomenon of the terpolymer using dynamic or static light scattering (DLS or SLS) and NMR spectrometry.

Fig. 2a shows the apparent molar mass (M_a) of terpolymer **1p** directly dispersed in water from the bulk, measured by SLS and DLS respectively. M_a (~ 40 kg.mol^{-1}) was close to that of single chains (M_w ≈ 35 kg.mol^{-1}), measured by SEC in DMF (Fig. S5, and Fig. S12 for the angular dependence of the scattered intensity). The hydrodynamic radius (R_h ≈ 6 nm (Fig. 2b)) also points to single chains compared to aggregates. Note that some kinetically frozen systems cannot reorganize upon direct dissolution giving structures similar to those formed in the bulk [59]. In order to check this possibility, the terpolymer was first dissolved in DMSO (a good solvent for the whole polymer that "erases" the thermal history of the polymer) before adding water under stirring ("DMSO route"). Both M_a and R_h remained the same using this preparation process (Fig. 2a and b). This shows that the terpolymer formed unimers in aqueous solution whatever the preparation route and that the 4F-AZO groups do not bridge polymer chains inter-molecularly since no evolution of the M_a was recorded with increasing the concentration. Note that the M_a and R_h of the terpolymer in water are also independent of the configuration of the 4F-AZO group. TEM characterization further confirmed this conclusion (Fig. S8) by the observation of monodisperse particles of diameter ~ 5-10 nm. However, the objects are too small and the contrast too low for extracting a reliable size distribution from the TEM images.

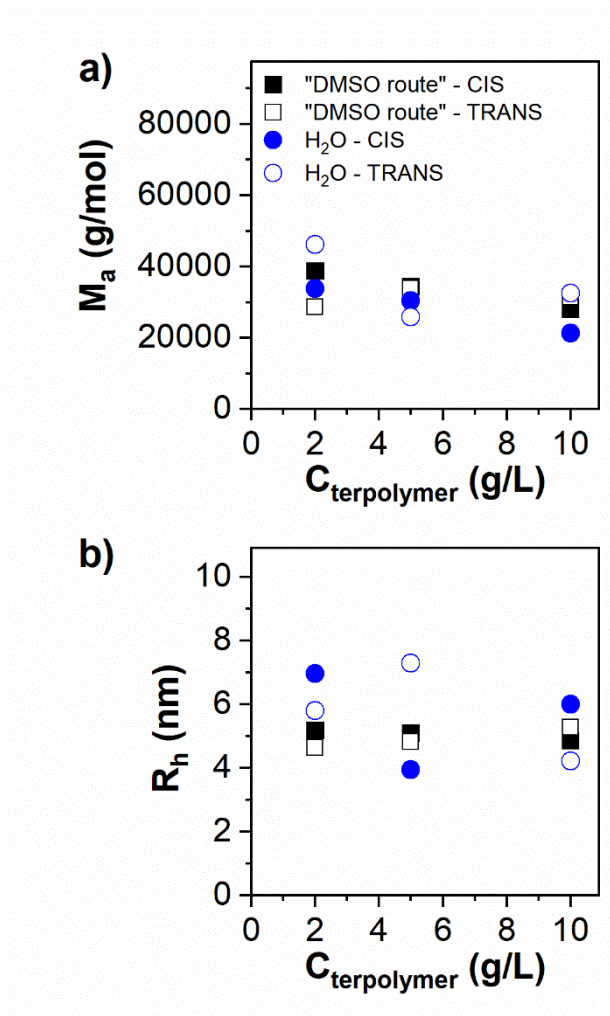

Fig. 2. Characterization of protected terpolymer **1p** in water. Concentration dependence of a) the apparent molar mass (M_a) b) the hydrodynamic radius (R_h) of the terpolymer prepared by direct dissolution in water (*cis*/*trans*) or via the "DMSO route" (*cis*/*trans*).

To further investigate the structure of the terpolymer in aqueous solution, NOESY NMR experiment was performed on a sample prepared using the "DMSO route" with deuterated solvents (DMSO-d_6/D_2O = 1:10 $_{v/v}$ %). Fig. 3a shows a correlation peak between the aromatic protons of the azobenzene (at ~7 ppm) and the aliphatic protons of the terpolymer backbone (at ~1 ppm). Besides, no correlation peak was observed when the spectrum was recorded in pure DMSO-d_6 (Fig. 3b). Moreover, the signals of the aromatic protons were broader on the ^{1}H NMR spectra recorded in D_2O compared to that recorded in DMSO-d_6, indicating a lack of mobility of the 4F-AZO groups in water (Fig. 3a and b). The same behavior was observed for the *trans* form (Fig. S13). Therefore, the protected terpolymer self-assembled into unimolecular micelles in aqueous solutions, the hydrophobic 4F-AZO groups being aggregated onto the polymer backbone (Scheme 3).

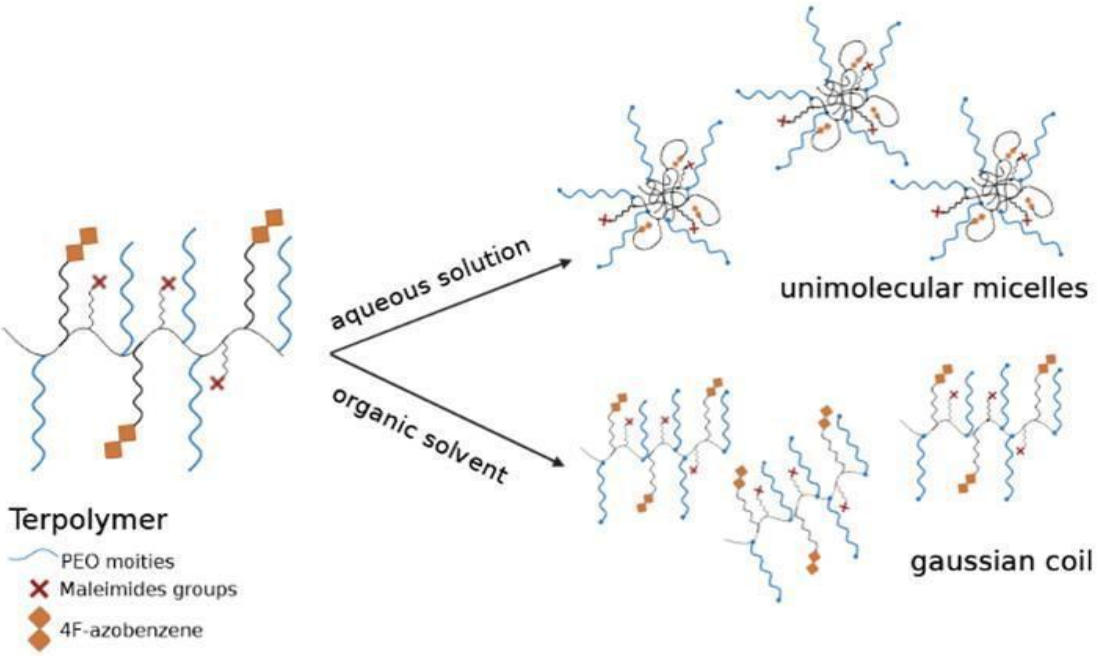

Scheme 3. Schematic representation of the terpolymer behavior in aqueous and organic solvent.

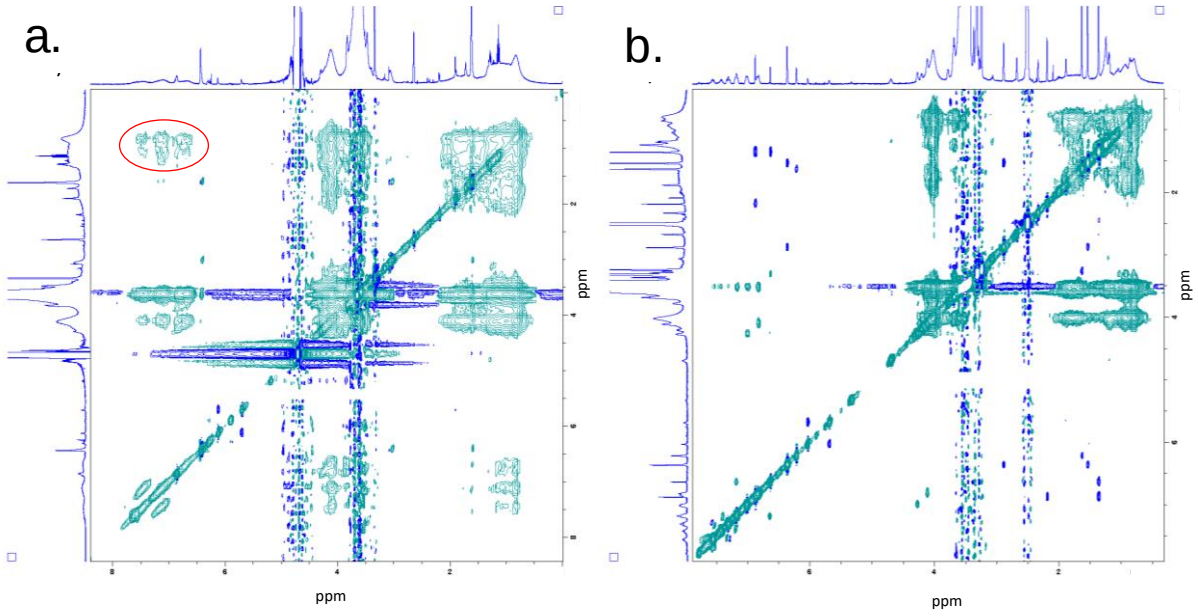

Fig. 3. NOESY map of the protected terpolymer in *cis* form in a) D_2O (using the DMSO route) and b) in DMSO-d_6.

In the literature, many examples of AZO-bearing polymers aqueous dispersions have been described. In early studies, this mainly dealt with amphiphilic polymers forming various self-assemblies in water [58, 60]. Illumination of the solutions led to change of size and/or morphology. To the best of our knowledge, the only discussed unimolecular micelle formation based on AZO-bearing polymers is the study described by Hao and coll. reporting an

association between an AZO-bearing polystyrene and β-CD-bearing poly(N-isopropylacrylamide) (PNIPAM) [61]. The term unimolecular micelle is suggested, based on the formed supramolecular association, it therefore involves more than one molecule by construction.

4F-AZO-PEO and the terpolymer exhibit very different self-assembly behaviors in water. A LCST is observed for the 4F-AZO-PEO which is not present for the terpolymer, presumably due to the higher ratio of PEO chain compared to the hydrophobic parts. Furthermore, whereas 4F-AZO-PEO formed micelles at 1.5 mM in water at 4°C [35], the terpolymer formed only unimolecular micelles at higher concentrations, ca. 3 mM eq. AZO. The interaction between 4F-AZO groups and the polymer chain is expected to play a crucial role in this observed behavior. The micelle formation for 4F-AZO-PEO in water can be explained by intermolecular attractions between fluorophenyl groups which are slightly more attractive than those of the hydro analogs. This is due mainly to the increased non-directional van der Waals attraction component [62-63]. In the case of the terpolymer, the interactions between 4F-AZO and the poly(methacrylate) main chain are favored compared to 4F-AZO/4F-AZO interactions. This proves that wrapping the poly(methacrylate) chains around the very hydrophobic 4F-AZO moieties is energetically less demanding than gathering 4F-AZO groups into micellar aggregates.

The behavior of the terpolymer also differs noticeably from that of hydrogenated copolymers reported in the literature. Copolymers bearing AZO-based hydrophobic moieties or blocks and poly(acrylic acid)(PAA) [44, 64-65], PEO [66] or poly(dimethyl aminoethyl methacrylate) (PDMAEMA) [43] hydrophilic chains were shown to self-assemble into micellar aggregates in aqueous-based solvents. In the case of strongly associated and, thus, frozen aggregates, UV-induced *trans*/*cis* switching did not modify the structures [43, 65]. However, reversible modifications and, sometimes, disruption of the aggregates under UV irradiation were reported when the amount of organic cosolvent was sufficient to allow reorganization of the self-assemblies [44, 64-65]. To the best of our knowledge, the formation of unimolecular micelles, and thus, the inability to form intermolecular aggregates, has not been reported before with polymers bearing hydrogenated-AZO moieties contrary to what we observed with 4F-AZO groups.

3.4 Interaction with β-CD-bearing molecules

Self-assemblies of AZO molecules in the presence of cyclodextrin-based molecules are regularly assessed as they enable additional functions such as drug release [67] beside morphology change upon illumination [68]. It was also already shown that *trans*-4F-AZO-PEO and *cis*-4F-AZO-PEO both form 1:1 inclusion complexes with β-CD in water, with affinity constants respectively at 1620 and 7120 M^{-1}.[35] In the literature, *trans*-AZOs are often described with a better affinity for β-CD versus the *cis* form. However, the few published 4F-AZOs seem to work in a reverse manner in aqueous solutions, the *cis* form exhibiting a higher affinity constant compared to the *trans* form [31, 69]. It is also noteworthy that in comparison, the hydrogenated *trans*-H-AZO-PEO exhibited an association constant with β-CD of 3000 M^{-1} and the *cis* form one at 4000 M^{-1} in water [34]. The main driving factor of *cis* isomer complexation results in a tight fit between the fluorinated guest and the β-CD cavity through Van der Waals interactions

whereas in the case of *trans* isomer the complexation result in hydrophobic interaction between the fluorinated azobenzene moiety and the cavity with a relatively high conformational and transitional flexibility [31]. The association between the protected terpolymer **1p** and β-CD was examined and compared with those of 4F-AZO-PEO and β-CD. In the case of 4F-AZO-PEO, the presence of inclusion complexes is easily observed by ^{1}H NMR through a shift of the peaks from the aromatic protons by a downfield shift with the increase of the quantity of β-CD [35]. However, in the case of the protected terpolymer **1p**, no shift was observed by ^{1}H or ^{19}F NMR (Fig. S14), indicating the absence of interaction between the 4F-AZO moieties and β-CD. The same conclusion was drawn from UV-visible spectra performed with increasing amounts of β-CD (data not shown). Therefore, the formation of unimolecular micelles for the terpolymer and, especially, the existing interaction between the fluorinated AZO and the polymer main chain prohibited the interaction between AZO and β-CD. This is a completely unexpected result compared to the literature where examples of hydrogenated AZO-bearing polymers are often described for their interaction with β-CD [16-17, 39, 67].

Because the protected terpolymer was able to form unimolecular micelles and thus isolated the 4F-AZO group from water, we evaluated whether the inclusion complex could be "forced" to be formed in different conditions minimizing the presence of water. For this, DMSO/water mixtures were assessed, as well as mixing of the terpolymer with β-CD without any solvent in a blender, following processes of mechanochemistry.[70] However, none of these conditions enabled us to observe without any doubt the formation of an inclusion complex. It seems that the strong interactions between the 4F-AZO and the polymer backbone completely inhibits any formation of complexes with the β-CD. To the best of our knowledge, such inhibition was never reported before.

3.5 To biological applications

Formation of bioconjugates

Maleimide functions are well-known to be involved in chemical reaction leading to the formation of hydrogels [71] or bioconjugates [72]. To that end, the maleimide groups were deprotected *via* a retro-Diels Alder (rDA) reaction by heating at the boiling temperature of dimethylfuran (94°C). The removal of the maleimide protection was verified by ^{1}H NMR (Fig. S6) showing the disappearance of the methyl peaks at 6.2 and 6.3 ppm simultaneously to the increase of the maleimide protons at 6.7 ppm.

The reactivity of maleimide groups was used to obtain bioconjugates by grafting two different thiol-bearing biomolecules: a biotinyl-PEO-SH and a peptide. They were grafted to the terpolymer via Michael maleimide-thiol reaction in aqueous media. A peptide with the GCREIPESLRAGERC sequence with two cysteine amino acids was successfully grafted to the terpolymer by simple mixing at room temperature (Fig. S15). On the ^{1}H NMR spectrum, the signals at 6.8 (maleimide protons) and 2.95 ppm (methylene protons in L-cysteine) decreased with the addition of peptide, as thiols consumed the maleimide functions. The NMR spectrum of the final product after dialysis and freeze drying was a combination of both the terpolymer and the peptide spectra proving the covalent bonding between both molecules. Another conjugate was formed as an example, using biotin-PEO-SH. Fig. S16 and S17 show the

disappearance of the maleimide signal with the addition of thiol bearing molecules. The triplet signal at 2.65 ppm collapses as soon as the biotin-PEO-SH is added to the terpolymer and the signals around 2.9 ppm are modified by the appearance of S-C bond characteristic signals. Maleimide moieties on the terpolymer are still accessible to easily react with thiols and enable the grafting of bioactive molecules in aqueous solution.

Formation of hydrogel

A hydrogel was prepared in water *via* maleimide-thiol reaction involving the deprotected terpolymer **1** (C=10 $_{wt}$%) and a tetra-thiol-PEO (Fig. 4a). The maleimide groups were thus deprotected following the same procedure than above. The formation of the hydrogel was followed by *in situ* rheometry (Fig. 4b). A fast and efficient cross-linking was obtained in a few tens of seconds. The swelling ratio of the obtained hydrogel was measured in ultra-pure water and the plateau was reached at 80% of swelling after 35 h of incubation at 6°C. (Fig. S18). Uniaxial unconfined compression was implemented on the swollen hydrogel (Fig. S9). The Young modulus obtained was around 22 kPa, which is in the range of typical biological tissues such as muscle, heart or breast.

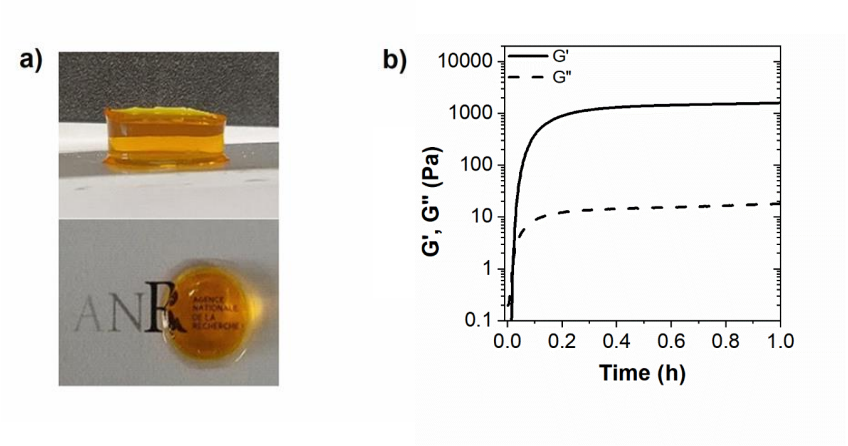

Fig. 4. a) Hydrogels made from the deprotected terpolymer via the thiol-maleimide reaction. b) Kinetics of the storage (G') (line) and the loss (G") (dash line) moduli of the hydrogel with time upon formation.

The hydrogel was then exposed to various cycles of green (530 nm) and blue (415 nm) light and *in situ* rheometry performed. No evolution of G' or G" was observed upon light exposure (Fig. S19). Although the photo-switch occurred at the molecular level (Fig. S20), the mechanical properties of the macroscopic hydrogel were not affected. Some studies reported a macroscopic response of AZO-based hydrogels. Rosales et al. obtained a very small change in the mechanical properties (ca. 3% change of G') upon illumination of a PEG/AZO-peptide hydrogel [13]. Similar observations were reported by Zhao et al., where G' varied from 370 to 360 Pa in water, while no change was observed in DMSO for a PEG/AZO-F [12]. Li et al. observed an increase of 15% of the photostrain (ΔL/L0) for a segregated PEG/AZO-diacrylate while 2% was usually obtained for random systems [73]. It is essential to note that these results were all obtained with systems containing AZO groups in the main chain of the polymer, meaning that it belonged to the links responsible for the chemical crosslinking. This shows that the central position of the AZO group is essential to induce a macroscopic change, either

through a stronger torque effect or to a suitable modification of chemical group interactions. The result obtained with our hydrogel is therefore not surprising since the 4F-AZO group was found to be unable to form intermolecular clusters.

Finally, hydrogels incorporating both the 4F-AZO terpolymer and β-CD molecules were assessed (scheme 4). For this, a hydrophilic cyclodextrin functionalized with several maleimide groups was synthesized (Schemes S3-S4 and Suppl. Info for the description, Fig. S21-S22). Different formulations of the 4-component (terpolymer, maleimide-β-CD-PEO and two and four-armed thiol-terminated PEG) hydrogels were prepared with stiffness in the range of 4 to 25 kPa (scheme S5 and Fig.S23). Cryo-SEM imaging of hydrogels revealed pore size around 10 nanometers (Fig. S24). It has been verified that these gels did not release any cytotoxic molecules in their surrounding medium (Fig. S25). As anticipated from the experiments without CD and those revealing the absence of complexation with the polymer, their modulus, which was measured by AFM force mapping, did not exhibit any change upon illumination (Fig. S26).

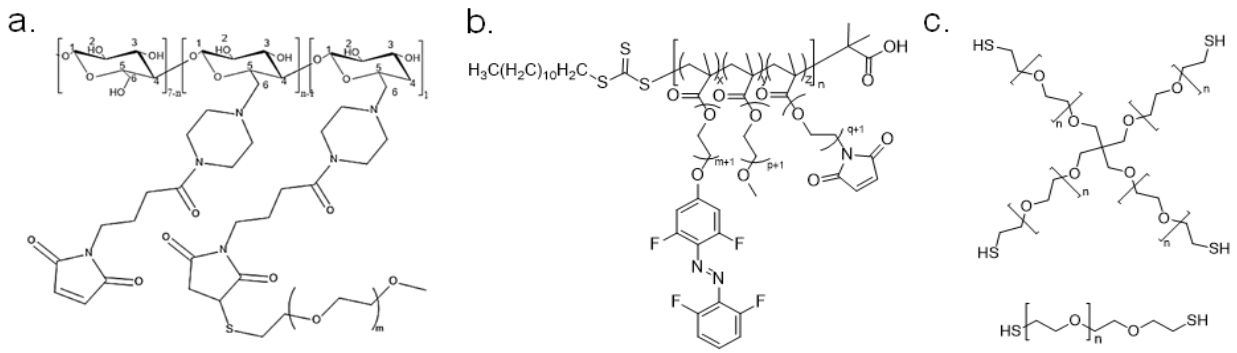

Scheme 4. Molecules used to form the hydrogels. a. β-CD derivative bearing reactive maleimide moieties and PEO side chains, b. terpolymer, c. two and four-armed thiol-terminated PEG.

To complete the overall comparison with literature, Table 2 presents examples of hydrogels incorporating AZO and cyclodextrin moieties in the formulation. The AZO@CD inclusion complex constitutes for most cases a physical crosslinking. Obviously for such systems the AZO groups have to be pendant and available for the CD, thus they are never in the main chain of the polymer. Several points are noteworthy:

- for most cases, this physical crosslinking is the only one present in the system. These systems are therefore expected to lose their mechanical resistance upon illumination if all complexes dissociate, leading to flowing systems [17, 39-40, 42, 45-47, 49, 74-76].

- if present, the additional chemical crosslinking is most often due to an independent polymer network [38, 76-77]. However, in these cases, no modulus change is presented. Only in our former study was a real common network incorporating both β-CD and AZO presented [78]. In this case, we were able to observe a 50% change in the modulus.

- when the storage modulus is given, in most cases, the value is below 1kPa, except in our former study [78].

Table 2. Examples of AZO-macromolecular hydrogels in the presence of cyclodextrin and their macroscopic response upon illumination. CMC Carboxymethylcellulose, PAA poly(acrylic acid), PAm polyacrylamide, PNIPAM poly(N-isopropyl acrylamide), CMC carboxymethylcellulose

AZO type	Gel structure	Gel formation method	Photoresponse	Application	Ref
AZO-H	PAAmAZO-PNIPAM-BAAm/ α-CD	Radical polymerization, chemical crosslinking only	Change of curvature	Change of curvature	[77]
AZO-H	Lignin-α-CD/AZO-guanidine/PAA	Physical crosslinking only, by AZO@CD and guanidine/PAA	Modulus change from 120 to 20 Pa		[74]
AZO-H	PAA-PAZO/curdlan-α-CD	Physical crosslinking only, by AZO@CD	Rheometry, viscosity decrease of ca. 80%		[75]
AZO-H	CMC/β-CD dimer	Physical crosslinking only, by AZO-H@β-CD	Modulus change from 65 to 30 Pa	Self-healing, drug delivery	[45]
AZO-H	HA-AZO/HA-β-CD	Physical crosslinking only, by AZO@CD	Modulus change from 155 to 140 Pa	EGF release	[47]
AZO-H	PAAm-AZO/Alg-β-CD	Physical crosslinking by AZO@CD + chemical crosslinking by BAAm network		Self-healing	[38]
AZO-H	PAA-AZO/PAA-β-CD	Physical crosslinking only, by AZO@CD		Self-healing	[39]
AZO-H	PAA-β-CD/PAA-AZO/PVA	Physical crosslinking only, by AZO@CD	Gel to sol upon illumination	Pollutant removal	[49]
AZO-H	PAm-AZO/PMA-β-CD	Physical crosslinking only, by AZO@CD		Photocontrolled anti-bacterial surface	[40]
AZO-H	HA-AZO/HA-β-CD	Physical crosslinking only, by AZO@CD	Modulus change from 1000 to 600 Pa	Protein release and substrate for mechanobiology	[17]

AZO-H	PNIPAM-PAZO/β-CD dimer	Physical crosslinking only, by AZO@CD	Rheometry, viscosity decrease of ca. 90%		[42]
AZO-H	PAAm-PAZO/β-CD nanogel	Physical crosslinking only, by AZO@CD Simultaneous radical polymerization		Self-healing hydrogel	[76]
AZO-H	AZO-dimaleimide/β-CD dimaleimide/ PEG-SH	Chemical and physical crosslinking	Modulus change from 30 to 14 kPa		[78]
AZO-OMe	PAA-AZO-OMe/β-CD dimer	Physical crosslinking only, by AZO-OMe@β-CD	Modulus change from 40 to 0.3 Pa	release	[46]

Conclusion

The work presented here has shown the access to a maleimide-functionalized terpolymer which can be used as a platform for building hydrogels or bioconjugates. However, several crucial points need to be taken into account. First the synthesis by itself constituted a challenge because of the temperature-sensitive protected maleimide group. Only RAFT performed at 30 °C enabled a successful synthesis without altering any functional groups. The obtained terpolymer was shown to form unimolecular micelles in water, an unprecedented phenomenon for AZO-bearing polymers.

Furthermore, an important point is the absence of macroscopic response of the hydrogel upon successive green or blue light illuminations. In the literature, photo-responsive morphology changes of systems bearing hydrogenated AZO moieties have been very often shown. These have been often linked to the change of polarity between the *cis* and *trans* forms. In the present system, the absence of change could be linked to a lack of modification of the polarity between both isomers, due to the high hydrophobicity of the fluorine atoms. These results should be kept in mind for researchers planning to use fluorinated azobenzenes. For future studies, a balance between the needed stimulation in the visible range and the azobenzene accessibility should be assessed before developing a system including tetra-*ortho substituted*-azobenzene polymers.

Author Contributions

C. Courtine investigation, P.-L. Brient investigation, I. Hamouda, investigation, P. Lavedan investigation, J.-L. Putaux investigation, C. Chatard methodology, N. Pataluch investigation, C. Galès supervision, A.-F. Mingotaud conceptualization, funding acquisition, supervision, N. Lauth de Viguerie conceptualization, methodology, supervision and E. Nicol conceptualization, methodology, supervision. All authors contributed to the writing of the original draft

Conflicts of interest

There are no conflicts to declare.

Acknowledgements

The authors acknowledge the French National Research Agency for funding (Gellight project ANR-18-CE06-0027). We acknowledge the EU for financial support (FEDER-35477: Nano-objets pour la biotechnologie) for the DSC instrument and the NanoBio-ICMG platform (UAR 2607, Grenoble) for granting access to the Electron Microscopy facility.

References

1. Bandara, H. M. D.; Burdette, S. C., Photoisomerization in different classes of azobenzene. *Chemical Society Reviews* **2012,** *41* (5), 1809-1825.
2. Weinstain, R.; Slanina, T.; Kand, D.; Klán, P., Visible-to-NIR-Light Activated Release: From Small Molecules to Nanomaterials. *Chemical Reviews* **2020,** *120* (24), 13135-13272.
3. Weis, P.; Wu, S., Light-Switchable Azobenzene-Containing Macromolecules: From UV to Near Infrared. *Macromolecular Rapid Communications* **2018,** *39* (1), 1700220.
4. Yang, Z.; Liu, Z.; Yuan, L., Recent Advances of Photoresponsive Supramolecular Switches. *Asian Journal of Organic Chemistry* **2021,** *10* (1), 74-90.
5. Sun, S.; Liang, S.; Xu, W.-C.; Xu, G.; Wu, S., Photoresponsive polymers with multi-azobenzene groups. *Polymer Chemistry* **2019,** *10* (32), 4389-4401.
6. Dong, R.; Zhu, B.; Zhou, Y.; Yan, D.; Zhu, X., Reversible photoisomerization of azobenzene-containing polymeric systems driven by visible light. *Polymer Chemistry* **2013,** *4* (4), 912-915.
7. Ren, H.; Chen, D.; Shi, Y.; Yu, H.; Fu, Z., A carboxylic azo monomer and its homopolymer: synthesis, self-organization and fluorescence behaviour in solution. *Polymer Chemistry* **2015,** *6* (2), 270-277.
8. Wen, W.; Chen, A., The self-assembly of single chain Janus nanoparticles from azobenzene-containing block copolymers and reversible photoinduced morphology transitions. *Polymer Chemistry* **2021,** *12*, 2447-2456.
9. Luo, P.-F.; Xiang, S.-L.; Li, C.; Zhu, M.-Q., Photomechanical polymer hydrogels based on molecular photoswitches. *Journal of Polymer Science* **2021,** *59* (20), 2246-2264.
10. Mohamadhoseini, M.; Mohamadnia, Z., Supramolecular self-healing materials via host-guest strategy between cyclodextrin and specific types of guest molecules. *Coordination Chemistry Reviews* **2021,** *432*, 213711.
11. Rizzo, F.; Kehr, N. S., Recent Advances in Injectable Hydrogels for Controlled and Local Drug Delivery. *Advanced Healthcare Materials* **2021,** *10* (1), 2001341.
12. Zhao, F.; Bonasera, A.; Nöchel, U.; Behl, M.; Bléger, D., Reversible Modulation of Elasticity in Fluoroazobenzene-Containing Hydrogels Using Green and Blue Light. *Macromolecular Rapid Communications* **2017**, 1700527-n/a.
13. Rosales, A. M.; Mabry, K. M.; Nehls, E. M.; Anseth, K. S., Photoresponsive Elastic Properties of Azobenzene-Containing Poly(ethylene-glycol)-based Hydrogels. *Biomacromolecules* **2015,** *16*, 798-806.

14. Wang, D.; Zhao, W.; Wei, Q.; Zhao, C.; Zheng, Y., Photoswitchable Azobenzene/Cyclodextrin Host-Guest Complexes: From UV- to Visible/Near-IR-Light-Responsive Systems. *ChemPhotoChem* **2018,** *2* (5), 403-415.
15. Wang, H.; Zhu, C. N.; Zeng, H.; Ji, X.; Xie, T.; Yan, X.; Wu, Z. L.; Huang, F., Reversible Ion-Conducting Switch in a Novel Single-Ion Supramolecular Hydrogel Enabled by Photoresponsive Host–Guest Molecular Recognition. *Advanced Materials* **2019,** *31* (12), 1807328.
16. Gao, Y.; Guo, R.; Feng, Y.; Zhang, L.; Wang, C.; Song, J.; Jiao, T.; Zhou, J.; Peng, Q., Self-Assembled Hydrogels Based on Poly-Cyclodextrin and Poly-Azobenzene Compounds and Applications for Highly Efficient Removal of Bisphenol A and Methylene Blue. *ACS Omega* **2018,** *3* (9), 11663-11672.
17. Rosales, A. M.; Rodell, C. B.; Chen, M. H.; Morrow, M. G.; Anseth, K. S.; Burdick, J. A., Reversible Control of Network Properties in Azobenzene-Containing Hyaluronic Acid-Based Hydrogels. *Bioconjugate Chemistry* **2018,** *29* (4), 905-913.
18. Samanta, S.; Beharry, A. A.; Sadovski, O.; McCormick, T. M.; Babalhavaeji, A.; Tropepe, V.; Woolley, G. A., Photoswitching Azo Compounds in Vivo with Red Light. *Journal of the American Chemical Society* **2013,** *135* (26), 9777-9784.
19. Samanta, S.; McCormick, T. M.; Schmidt, S. K.; Seferos, D. S.; Woolley, G. A., Robust visible light photoswitching with ortho-thiol substituted azobenzenes. *Chemical Communications* **2013,** *49* (87), 10314-10316.
20. Bléger, D.; Schwarz, J.; Brouwer, A. M.; Hecht, S., o-Fluoroazobenzenes as Readily Synthesized Photoswitches Offering Nearly Quantitative Two-Way Isomerization with Visible Light. *Journal of the American Chemical Society* **2012,** *134* (51), 20597-20600.
21. Knie, C.; Utecht, M.; Zhao, F.; Kulla, H.; Kovalenko, S.; Brouwer, A. M.; Saalfrank, P.; Hecht, S.; Bléger, D., ortho-Fluoroazobenzenes: Visible Light Switches with Very Long-Lived Z Isomers. *Chemistry – A European Journal* **2014,** *20* (50), 16492-16501.
22. Qian, S.; Li, S.; Xiong, W.; Khan, H.; Huang, J.; Zhang, W., A new visible light and temperature responsive diblock copolymer. *Polymer Chemistry* **2019,** *10* (36), 5001-5009.
23. Gao, M.; Kwaria, D.; Norikane, Y.; Yue, Y., Visible-light-switchable azobenzenes: Molecular design, supramolecular systems, and applications. *Natural Sciences* **2023,** *3* (1), e220020.
24. Bian, Q.; Jin, M.; Chen, S.; Xu, L.; Wang, S.; Wang, G., Visible-light-responsive polymeric multilayers for trapping and release of cargoes via host–guest interactions. *Polymer Chemistry* **2017,** *8* (36), 5525-5532.
25. Wang, D.; Wagner, M.; Butt, H.-J.; Wu, S., Supramolecular hydrogels constructed by red-light-responsive host-guest interactions for photo-controlled protein release in deep tissue. *Soft Matter* **2015,** *11* (38), 7656-7662.
26. Dong, M.; Babalhavaeji, A.; Samanta, S.; Beharry, A. A.; Woolley, G. A., Red-Shifting Azobenzene Photoswitches for in Vivo Use. *Accounts of Chemical Research* **2015,** *48* (10), 2662-2670.
27. Agnetta, L.; Bermudez, M.; Riefolo, F.; Matera, C.; Claro, E.; Messerer, R.; Littmann, T.; Wolber, G.; Holzgrabe, U.; Decker, M., Fluorination of Photoswitchable Muscarinic Agonists Tunes Receptor Pharmacology and Photochromic Properties. *Journal of Medicinal Chemistry* **2019,** *62* (6), 3009-3020.
28. Kerckhoffs, A.; Bo, Z.; Penty, S. E.; Duarte, F.; Langton, M. J., Red-shifted tetra-ortho-halo-azobenzenes for photo-regulated transmembrane anion transport. *Organic & Biomolecular Chemistry* **2021,** *19* (41), 9058-9067.
29. Nie, C.; Liu, C.; Sun, S.; Wu, S., Visible-Light-Controlled Azobenzene-Cyclodextrin Host-Guest Interactions for Biomedical Applications and Surface Functionalization. *ChemPhotoChem* **2021,** *5* (10), 893-901.
30. Kumar, K.; Knie, C.; Bléger, D.; Peletier, M. A.; Friedrich, H.; Hecht, S.; Broer, D. J.; Debije, M. G.; Schenning, A. P. H. J., A chaotic self-oscillating sunlight-driven polymer actuator. *Nature communications* **2016,** *7* (1), 11975.
31. Huang, H.; Juan, A.; Katsonis, N.; Huskens, J., Competitive inclusion of molecular photo-switches in host cavities. *Tetrahedron* **2017,** *73* (33), 4913-4917.
32. Brandrup, J.; Immergut, E. H., *Polymer Handbook*. 3rd edition ed.; John Wiley & Sons: 1989.

33. Ravasco, J. M. J. M.; Faustino, H.; Trindade, A.; Gois, P. M. P., Bioconjugation with Maleimides: A Useful Tool for Chemical Biology. *Chemistry – A European Journal* **2019,** *25* (1), 43-59.
34. Royes, J.; Courtine, C.; Lorenzo, C.; Lauth-de Viguerie, N.; Mingotaud, A.-F.; Pimienta, V., Quantitative Kinetic Modeling in Photoresponsive Supramolecular Chemistry: The Case of Water-Soluble Azobenzene/Cyclodextrin Complexes. *The Journal of Organic Chemistry* **2020,** *85* (10), 6509-6518.
35. Courtine, C.; Hamouda, I.; Pearson, S.; Billon, L.; Lavedan, P.; Ladeira, S.; Micheau, J.-C.; Pimienta, V.; Nicol, E.; Lauth de Viguerie, N.; Mingotaud, A.-F., Photoswitchable assembly of long-lived azobenzenes in water using visible light. *Journal of Colloid and Interface Science* **2023,** *629*, 670-684.
36. Porsch, C.; Hansson, S.; Nordgren, N.; Malmström, E., Thermo-responsive cellulose-based architectures: tailoring LCST using poly(ethylene glycol) methacrylates. *Polymer Chemistry* **2011,** *2* (5), 1114-1123.
37. Chan, N.; Jung, H. W.; Noh, S. M.; Oh, J. K., Functional amphiphilic oligo(ethylene oxide) methacrylate-based block copolymers: synthesis by an activator regenerated by electron transfer process for atom transfer radical polymerization and aqueous micellization. *Polymer International* **2014,** *63* (5), 858-867.
38. He, F.; Wang, L.; Yang, S.; Qin, W.; Feng, Y.; Liu, Y.; Zhou, Y.; Yu, G.; Li, J., Highly stretchable and tough alginate-based cyclodextrin/Azo-polyacrylamide interpenetrating network hydrogel with self-healing properties. *Carbohydrate Polymers* **2021,** *256*, 117595.
39. Han, W.; Liu, Z.; Wang, S.; Ji, Y.; Zhang, X., Construction of a Novel Photoresponsive Supramolecular Fluorescent Hydrogel through Host-Guest Interaction between β-Cyclodextrin and Azobenzene. *ChemistrySelect* **2020,** *5* (7), 2300-2305.
40. Ni, Y.; Zhang, D.; Wang, Y.; He, X.; He, J.; Wu, H.; Yuan, J.; Sha, D.; Che, L.; Tan, J.; Yang, J., Host–Guest Interaction-Mediated Photo/Temperature Dual-Controlled Antibacterial Surfaces. *ACS Applied Materials & Interfaces* **2021,** *13* (12), 14543-14551.
41. Lee, D. C.; Guye, K. N.; Paranji, R. K.; Lachowski, K.; Pozzo, L. D.; Ginger, D. S.; Pun, S. H., Dual-Stimuli Responsive Single-Chain Polymer Folding via Intrachain Complexation of Tetramethoxyazobenzene and β-Cyclodextrin. *Langmuir* **2021,** *37* (33), 10126-10134.
42. Guan, Y.; Zhao, H.-B.; Yu, L.-X.; Chen, S.-C.; Wang, Y.-Z., Multi-stimuli sensitive supramolecular hydrogel formed by host-guest interaction between PNIPAM-Azo and cyclodextrin dimers. *RSC Advances* **2014,** *4* (10), 4955-4959.
43. Ravi, P.; Sin, S. L.; Gan, L. H.; Gan, Y. Y.; Tam, K. C.; Xia, X. L.; Hu, X., New water soluble azobenzene-containing diblock copolymers: synthesis and aggregation behavior. *Polymer* **2005,** *46* (1), 137-146.
44. Wang, G.; Tong, X.; Zhao, Y., Preparation of Azobenzene-Containing Amphiphilic Diblock Copolymers for Light-Responsive Micellar Aggregates. *Macromolecules* **2004,** *37* (24), 8911-8917.
45. Kim, Y.; Jeong, D.; Shinde, V. V.; Hu, Y.; Kim, C.; Jung, S., Azobenzene-grafted carboxymethyl cellulose hydrogels with photo-switchable, reduction-responsive and self-healing properties for a controlled drug release system. *International Journal of Biological Macromolecules* **2020,** *163*, 824-832.
46. Yan, H.; Jiang, Q.; Wang, J.; Cao, S.; Qiu, Y.; Wang, H.; Liao, Y.; Xie, X., A triple-stimuli responsive supramolecular hydrogel based on methoxy-azobenzene-grafted poly(acrylic acid) and β-cyclodextrin dimer. *Polymer* **2021,** *221*, 123617.
47. Zhao, W.; Li, Y.; Zhang, X.; Zhang, R.; Hu, Y.; Boyer, C.; Xu, F.-J., Photo-responsive supramolecular hyaluronic acid hydrogels for accelerated wound healing. *Journal of Controlled Release* **2020,** *323*, 24-35.
48. Zou, L.; Addonizio, C. J.; Su, B.; Sis, M. J.; Braegelman, A. S.; Liu, D.; Webber, M. J., Supramolecular Hydrogels via Light-Responsive Homoternary Cross-Links. *Biomacromolecules* **2021,** *22* (1), 171-182.
49. Hou, N.; Wang, R.; Wang, F.; Bai, J.; Zhou, J.; Zhang, L.; Hu, J.; Liu, S.; Jiao, T., Fabrication of Hydrogels via Host–Guest Polymers as Highly Efficient Organic Dye Adsorbents for Wastewater Treatment. *ACS Omega* **2020,** *5* (10), 5470-5479.

50. Si, X.; Ma, S.; Xu, Y.; Zhang, D.; Shen, N.; Yu, H.; Zhang, Y.; Song, W.; Tang, Z.; Chen, X., Hypoxia-sensitive supramolecular nanogels for the cytosolic delivery of ribonuclease A as a breast cancer therapeutic. *Journal of Controlled Release* **2020,** *320*, 83-95.
51. Safar Sajadi, S. M.; Khoee, S., The simultaneous role of porphyrins' H- and J- aggregates and host–guest chemistry on the fabrication of reversible Dextran-PMMA polymersome. *Scientific Reports* **2021,** *11* (1), 2832.
52. Jia, L.; Kilbey, S. M.; Wang, X., Tailoring Azlactone-Based Block Copolymers for Stimuli-Responsive Disassembly of Nanocarriers. *Langmuir* **2020,** *36* (34), 10200-10209.
53. Becker, M. L.; Remsen, E. E.; Wooley, K. L., Diblock copolymers, micelles, and shell-crosslinked nanoparticles containing poly(4-fluorostyrene): Tools for detailed analyses of nanostructured materials. *Journal of Polymer Science Part A: Polymer Chemistry* **2001,** *39* (23), 4152-4166.
54. Zhu, M.; Zhang, X.; Wang, Y.; Wu, Y.; Wang, H.; Zhang, M.; Chen, Q.; Shen, Z.; Li, N., Novel anion exchange membranes based on quaternized diblock copolystyrene containing a fluorinated hydrophobic block. *Journal of Membrane Science* **2018,** *554*, 264-273.
55. Pugh, C.; Tang, C. N.; Paz-Pazos, M.; Samtani, O.; Dao, A. H., Correlation of Free Radical Copolymerization Behavior and Copolymer Properties with the Strength of π–π Stacking Interactions between Aromatic Fluorocarbons and Aromatic Hydrocarbons: Copolymerization of Styrene and Fluorinated Styrenes at the Two Extreme Levels of Fluorination. *Macromolecules* **2007,** *40* (23), 8178-8188.
56. Badi, N.; Lutz, J.-F., PEG-based thermogels: Applicability in physiological media. *Journal of Controlled Release* **2009,** *140* (3), 224-229.
57. Lutz, J.-F., Polymerization of oligo(ethylene glycol) (meth)acrylates: Toward new generations of smart biocompatible materials. *Journal of Polymer Science Part A: Polymer Chemistry* **2008,** *46* (11), 3459-3470.
58. Wu, S.; Wang, L.; Kroeger, A.; Wu, Y.; Zhang, Q.; Bubeck, C., Block copolymers of PS-b-PEO co-assembled with azobenzene-containing homopolymers and their photoresponsive properties. *Soft Matter* **2011,** *7* (24), 11535-11545.
59. Nicolai, T.; Colombani, O.; Chassenieux, C., Dynamic polymeric micelles versus frozen nanoparticles formed by block copolymers. *Soft Matter* **2010,** *6* (14), 3111-3118.
60. Su, W.; Zhao, H.; Wang, Z.; Li, Y.; Zhang, Q., Sphere to disk transformation of micro-particle composed

of azobenzene-containing amphiphilic diblock copolymers

under irradiation at 436 nm. *European Polymer Journal* **2007,** *43*, 657-662.
61. Gao, Z.; Chen, M.; Hu, Y.; Dong, S.; Cui, J.; Hao, J., Tunable assembly and disassembly of responsive supramolecular polymer brushes. *Polymer Chemistry* **2017,** *8* (18), 2764-2772.
62. Lorenzo, S.; Lewis, G. R.; Dance, I., Supramolecular potentials and embraces for fluorous aromatic molecules. *New Journal of Chemistry* **2000,** *24* (5), 295-304.
63. Kumar, A.; Mahato, J.; Dixit, M.; Patwari, G. N., Progressive Hydrophobicity of Fluorobenzenes. *The Journal of Physical Chemistry B* **2019,** *123* (47), 10083-10088.
64. Tong, X.; Wang, G.; Soldera, A.; Zhao, Y., How Can Azobenzene Block Copolymer Vesicles Be Dissociated and Reformed by Light? *The Journal of Physical Chemistry B* **2005,** *109* (43), 20281-20287.
65. Li, Y.; Deng, Y.; Tong, X.; Wang, X., Formation of Photoresponsive Uniform Colloidal Spheres from an Amphiphilic Azobenzene-Containing Random Copolymer. *Macromolecules* **2006,** *39* (3), 1108-1115.
66. Wang, D.; Ye, G.; Wang, X., Synthesis of Aminoazobenzene-Containing Diblock Copolymer and Photoinduced Deformation Behavior of its Micelle-Like Aggregates. *Macromolecular Rapid Communications* **2007,** *28* (23), 2237-2243.
67. Zhang, J.; Zhou, Z.-H.; Li, L.; Luo, Y.-L.; Xu, F.; Chen, Y., Dual Stimuli-Responsive Supramolecular Self-Assemblies Based on the Host–Guest Interaction between β-Cyclodextrin and Azobenzene for Cellular Drug Release. *Molecular Pharmaceutics* **2020,** *17* (4), 1100-1113.

68. Lu, Y.; Zou, H.; Yuan, H.; Gu, S.; Yuan, W.; Li, M., Triple stimuli-responsive supramolecular assemblies based on host-guest inclusion complexation between β-cyclodextrin and azobenzene. *European Polymer Journal* **2017,** *91*, 396-407.
69. Zhang, L.; Zhang, H.; Gao, F.; Peng, H.; Ruan, Y.; Xu, Y.; Weng, W., Host-guest interaction between fluoro-substituted azobenzene derivative and cyclodextrins. *RSC Advances* **2015,** *5* (16), 12007-12014.
70. Mura, P.; Faucci, M. T.; Parrini, P. L., Effects of Grinding with Microcrystalline Cellulose and Cyclodextrins on the Ketoprofen Physicochemical Properties. *Drug Development and Industrial Pharmacy* **2001,** *27* (2), 119-128.
71. Phelps, E. A.; Enemchukwu, N. O.; Fiore, V. F.; Sy, J. C.; Murthy, N.; Sulchek, T. A.; Barker, T. H.; García, A. J., Maleimide cross-linked bioactive PEG hydrogel exhibits improved reaction kinetics and cross-linking for cell encapsulation and in situ delivery. *Advanced materials (Deerfield Beach, Fla.)* **2012,** *24* (1), 64-70, 2.
72. Lutolf, M. P.; Tirelli, N.; Cerritelli, S.; Cavalli, L.; Hubbell, J. A., Systematic Modulation of Michael-Type Reactivity of Thiols through the Use of Charged Amino Acids. *Bioconjugate Chemistry* **2001,** *12* (6), 1051-1056.
73. Li, C.; Kim, H.; An, J.; Cho, M., Amplified photo-responses in sequentially polymerized azobenzene-containing polymer networks: the role of isomer interconnection. *Polymer Chemistry* **2020,** *11* (12), 1998-2005.
74. Gu, L.; Liu, X.; Dong, S.; Chen, Z.; Han, R.; He, C.; Wang, D.; Zheng, Y., Natural lignin nanoparticles: a promising nano-crosslinker for constructing fluorescent photoswitchable supramolecular hydrogels. *Polymer Chemistry* **2020,** *11* (11), 1871-1876.
75. Tamesue, S.; Takashima, Y.; Yamaguchi, H.; Shinkai, S.; Harada, A., Photoswitchable Supramolecular Hydrogels Formed by Cyclodextrins and Azobenzene Polymers. *Angewandte Chemie International Edition* **2010,** *49* (41), 7461-7464.
76. Yang, Q.; Wang, P.; Zhao, C.; Wang, W.; Yang, J.; Liu, Q., Light-Switchable Self-Healing Hydrogel Based on Host–Guest Macro-Crosslinking. *Macromolecular Rapid Communications* **2017,** *38* (6), 1600741-n/a.
77. Kuenstler, A. S.; Lahikainen, M.; Zhou, H.; Xu, W.; Priimagi, A.; Hayward, R. C., Reconfiguring Gaussian Curvature of Hydrogel Sheets with Photoswitchable Host–Guest Interactions. *ACS Macro Letters* **2020,** *9* (8), 1172-1177.
78. Royes Mir, J.; Coudret, C.; Roux, C.; Benoit-Marquié, F.; Cazalès, M.; Séverac, C.; Lorenzo, C.; Mingotaud, A.-F., Rational Hydrogel Formulation Leads to Reversible and Enhanced Photocontrolled Rigidity. *ChemPhotoChem* **2017,** *1* (7), 311-316.